Dynamic Shading Geometric Models for Buildings Based on Boundary Projection and Polygonal Boolean Operations

Changyue Li [1, *], Boxi Hou[1], Yixi Wan[1], Guanqiao Zhong[2], Kaifeng You[2]

{lizhangyue@stu.sau.edu.cn*}

College of Science, Shenyang Aerospace University, Shenyang, China[1]

College of Aeronautics and Astronautics, Shenyang Aerospace University, Shenyang, China[2]

Abstract. Addressing the complexity of evaluating dynamic shading performance in building energy-efficient design, this study constructs a full-time solar radiation geometric projection model. The research first establishes a calculation framework for ground-normal direct irradiance considering atmospheric path attenuation, based on solar trajectory theory combined with Beer-Lambert's law and the Kasten & Young correction formula. Subsequently, for complex cantilevered shading structures, an innovative boundary projection algorithm and polygonal Boolean operation logic were introduced. Computational geometry techniques enabled precise determination of the effective sun-exposed area of windows on all facades at any given time. Sensitivity analysis identified the cantilever depth of shading elements as the dominant geometric factor influencing shading performance and demonstrated the necessity of integrating horizontal and vertical shading designs. Experimental validation demonstrates that this model successfully intercepts 86% of radiant energy during the critical summer period, exhibiting significantly superior all-day shading performance compared to conventional standard solutions. This research provides a precise physical modeling foundation and parameter optimization pathway for building cooling and all-day dynamic shading strategies in low-latitude regions.

Keywords: Boundary projection; Boolean operations; Geometric optimization.

1 Introduction

As global building energy efficiency standards continue to rise, passive shading technology—a core climate-responsive design approach—plays a pivotal role in reducing building cooling energy consumption. However, traditional shading designs often rely on simplified midday calculations,

ICIAAI 2026, May 22-24, Singapore, Singapore

DOI 10.4108/eai.22-5-2026.2365363

neglecting the dynamic solar trajectory and seasonal radiation variations. This leads to severe overheating and glare issues during early morning and evening periods when the sun's angle is low. While prior research has examined the shading efficiency of fixed components, it often struggles with computational accuracy or fails to capture transient effects when evaluating real-time dynamic projections of complex shading geometries under high-dimensional parameter coupling. This section innovates by transforming the physical shading process into a geometric boundary projection problem based on vector algebra. For the first time, it employs polygonal Boolean operation algorithms to precisely subtract shadow areas, eliminating approximation errors inherent in traditional models. The overall research approach follows a logical sequence from dynamic solar azimuth calculation and atmospheric radiation attenuation modeling to geometric interference analysis of sunshades. It aims to provide theoretical support for the scientific layout and dimensional optimization of building facade shading facilities through refined geometric dynamics modeling [1-2].

The study first establishes a geometric reference for solar motion. By calculating solar declination, hour angle, and solar elevation and azimuth angles at different geographical latitudes, the model precisely locates the solar vector at any given moment [3-4]. For radiation intensity estimation, the model incorporates Beer-Lambert's law to describe the exponential attenuation of light intensity with atmospheric thickness, applying the Kasten & Young formula to correct for low elevation angles and thereby obtaining near-surface normal direct irradiance. This physical modeling process provides precise input boundaries for subsequent analysis of power reception in windows facing different orientations [5].

Shade Projection Area Calculation Based on Polygon Boolean Operations To address the dynamic shading of windows by sunshade components, this study proposes an analytical method based on geometric optical projection. By establishing a right-handed 3D coordinate system, the shading element boundary is mapped onto the geometric plane containing the window. The effective light-receiving area is defined as the Boolean difference between the window domain and the projected shadow domain [6-7]. Utilizing a specialized algorithm library for discretization, the model handles windows of various shapes—rectangular, circular, and triangular—enabling transient capture of effective light-receiving areas. This approach effectively overcomes the challenge of overlapping shadow calculations under complex geometric boundaries, significantly enhancing the computational accuracy of cumulative radiant energy throughout the day [8-9].

Sensitivity Analysis and Layout Optimization of Dynamic Shading Performance After clarifying the geometric mapping relationship, the study further explored the weighting of various shading panel parameters on shading performance. Sensitivity analysis indicates that overhang depth is the core variable determining shading effectiveness, while horizontal and vertical shading elements exhibit distinct complementary performance across different time periods. Based on these findings, a multivariate optimization model was developed to synergistically optimize window orientation and shading depth across facades, targeting minimization of average summer total radiation and shading material area. Results demonstrate that by finely adjusting the deflection angles of east- and north-facing windows in conjunction with optimized composite sunshades, summer radiation power can be reduced to 0.53 times or less of the unoptimized state [10].

2 Model Establishment and Solution

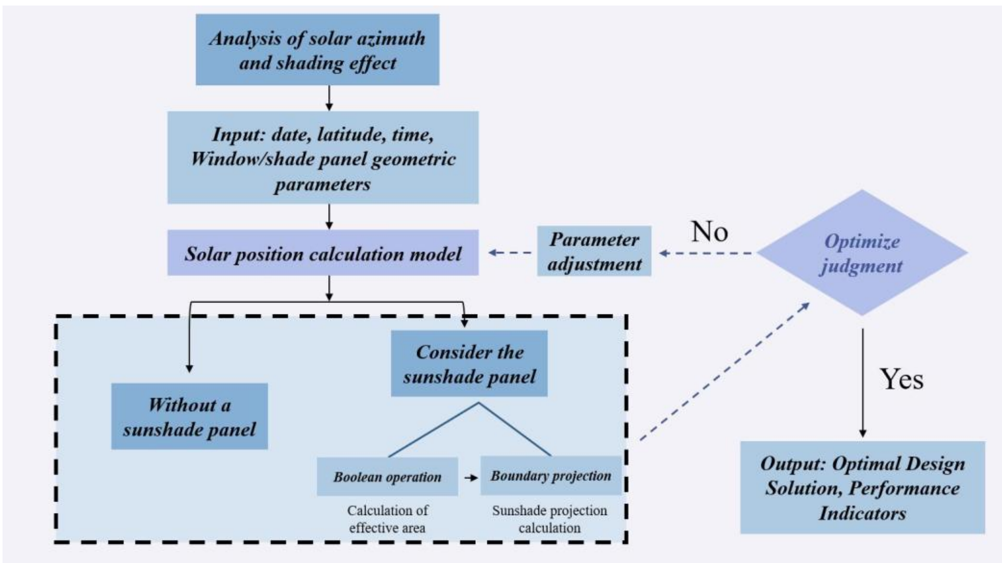

Figure 1 Conceptual framework

Conceptual framework is shown in figure 1.

2.1 Model Establishment

2.1.1 Determination of the solar azimuth angle

First, it is assumed that the sunlight radiating to the top of the Earth's atmosphere at any given moment is parallel light with constant power; at the same time, due to the significant difference between the Earth's revolution around the sun and the Earth's rotation period, the sun's trajectory in the sky throughout the day can be approximated as a circular arc. By calculating the solar altitude angle and azimuth angle, the solar azimuth at any given moment can be determined. For this, it is necessary to first calculate the solar declination angle and hour angle.

The solar hour angle, declination angle, altitude angle, and azimuth angle are shown in the following figure 2 and figure 3:

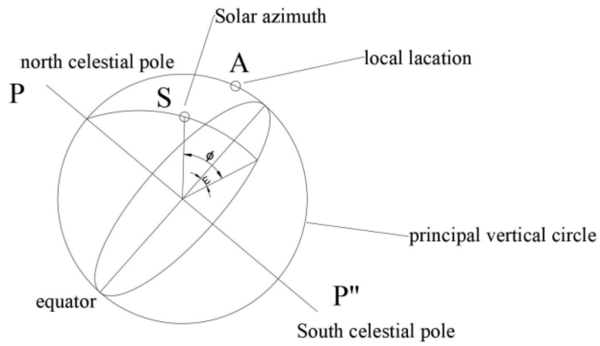

Figure 2 Schematic diagram of solar hour angle and declination angle

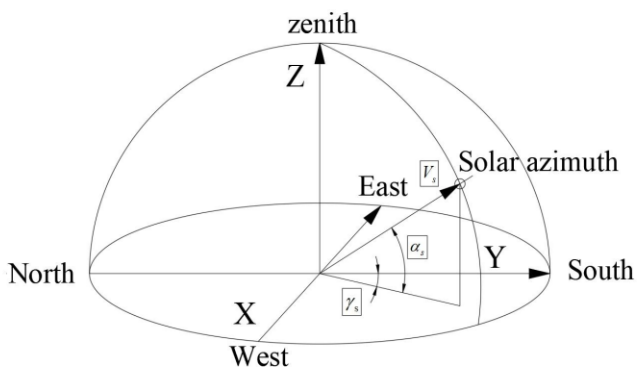

Figure 3 Diagram of solar altitude angle and azimuth angle

Solar declination angle ϕ is the angle between the line connecting the Sun and the Earth on a given date and the Earth's equatorial plane. Its calculation formula is as follows:

$$\sin\phi = \sin\frac{2\pi D}{365}\sin\left(\frac{2\pi}{360}23.45\right) \tag{1}$$

where D is the number of days from the first day after the spring equinox.

Solar hour angle ω is the angle of the Sun's rotation relative to the Earth caused by the Earth's rotation. Within a day, its size is approximately equal to the angle the Earth rotates. Its calculation formula is as follows:

$$\omega = \frac{\pi}{12}(\mathrm{LT} - 12) \tag{2}$$

where LT is the local time.

Therefore, the solar altitude angle and azimuth angle can be calculated at any location and time.

Solar altitude angle α_s is the angle between the incident sunlight and the ground plane at that location. Its calculation formula is as follows:

$$\sin\alpha_s = \cos\phi\cos\varphi\cos\omega + \sin\delta\sin\varphi \tag{3}$$

where φ is the local latitude (with North latitude as positive).

Solar Azimuth γ_s: This is the angle between the projection of the incident ray on the ground plane at this location and the due south direction (clockwise is positive). The calculation formula is as follows:

$$\cos\gamma_s = \frac{\sin\phi - \sin\alpha_s\sin\varphi}{\cos\alpha_s\cos\varphi} \tag{4}$$

2.1.2 Direct solar radiation intensity model without shading

According to the Beer-Lambert Law, the intensity of light decreases exponentially with atmospheric thickness as it passes through the atmosphere. Considering the case where the solar altitude angle is close to 0°, the Katten & Young formula can be used for correction to obtain the normal direct irradiance near the ground plane. DNI (unit: kW/m^2) refers to the solar radiation energy received per unit area per unit time on a plane perpendicular to the sun's rays on Earth. Its calculation formula is as follows:

$$\begin{aligned} &\mathrm{DNI} = G_0\left[a + b\exp\left(-\frac{c}{AW}\right)\right] \\ &a = 0.4237 - 0.00821(6 - H)^2 \\ &b = 0.5055 + 0.00595(6.5 - H)^2 \\ &c = 0.2711 + 0.01858(2.5 - H)^2 \\ &AW = \sin\alpha_s + 0.50572(\alpha_s + 6.07995)^{-1.6364} \end{aligned} \tag{5}$$

where G_0 is the solar constant, with a value of $1.366\ kW/m^2$, H is the altitude (unit: km), AW is the standard correction formula for atmospheric mass, α_s is the solar altitude angle.

Taking a south-facing window as an example, we assume the window can tilt eastward or westward at a certain angle (not exceeding 15°). We can set the normal vector of the plane containing the window $\vec{n}_1 = (\cos\gamma_1, \sin\gamma_1, 0)$, where γ_1 is the angle between the plane containing the window and the due south direction.

Then the radiation intensity received by the window per unit time is calculated as follows:

$$I_{t1} = \eta_{ln} \cdot \mathrm{DNI} \cdot A \cdot (\vec{s} \cdot \vec{n}_1) \tag{6}$$

where η_{in} is the transmittance of the glass to sunlight, A is the window area, $\vec{s}$ is the unit vector of the incident sunlight $(\cos\gamma_s\sin\alpha_s, \sin\gamma_s\sin\alpha_s, \cos\alpha_s)$.

Generally, a maximum of two facade windows can receive direct sunlight during the day. In areas north of the Tropic of Cancer and south of the North Pole, in summer, the sun's azimuth is north-northeast in the morning, due south at noon, and north-northwest in the evening; in winter, the sun's azimuth is north-northeast in the morning, due south at noon, and north-northwest in the evening.

We visualized the received power, angles with the sun's azimuth, and angles with the sun's altitude angle at any time of day for the south, north, and east facade windows, with a window area of $3m^2$, as shown in the figure below.

From the figure, we extract some meaningful points for later derivation:

(1) In summer, the solar radiation received mainly comes from the east, west, and north facades in the early morning and evening; the south facade receives less solar radiation due to the higher solar altitude angle.

(2) In winter, the solar radiation received mainly comes from the south facade near noon, and its intensity is particularly high due to the lower solar altitude angle; at the same time, the windows on the east facade receive a small amount of radiation from the south-southeast direction at sunrise; the north facade receives no solar radiation.

(3) The shading effect is significant when the solar azimuth or altitude angle is between 45 °and 90 °. In spring and autumn, the angles between the windows and the solar azimuth and altitude angles are moderate, making it suitable for studying the influence of the geometric parameters of south-facing and east-west-facing sunshades on the shading effect. In summer, the influence of the geometric parameters of north-facing sunshades on the shading effect can be studied. The schematic diagram of the received power, the angle with the solar azimuth and the angle with the solar elevation angle are shown in figure 4.

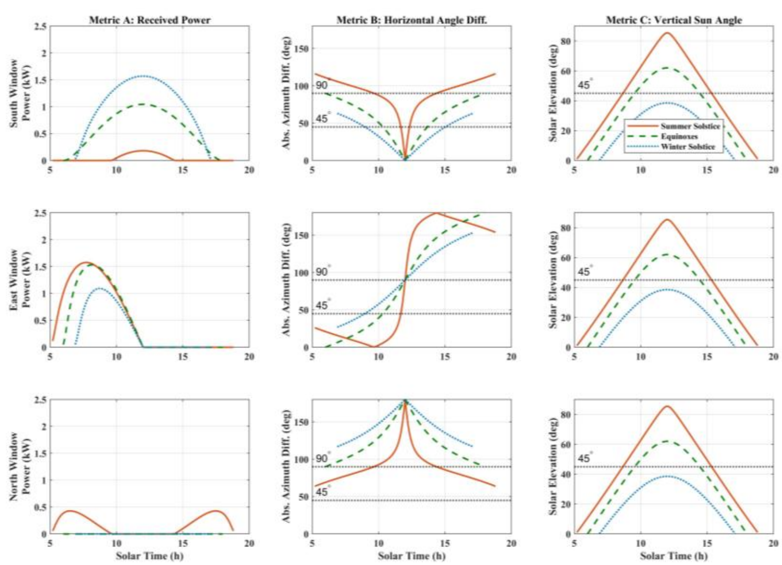

Figure 4 The schematic diagram of the received power, the angle with the solar azimuth and the angle with the solar elevation angle

2.1.3 Calculation of solar radiation intensity with horizontal and vertical shading

Let's take a rectangular window on the south facade as an example, as shown in the figure below. Let the window height be l, length be Y_0, the horizontal sunshade length be Y, and the width be k_1 times, from the top of the window h_1. The vertical sunshade is symmetrically distributed on both sides of the window, with its center and the center of the window at the same height l_1, with a width equal to the height of the window k_2 times, from the side of the window y_1. Due to symmetry, we only need to study the situation between sunrise and noon.

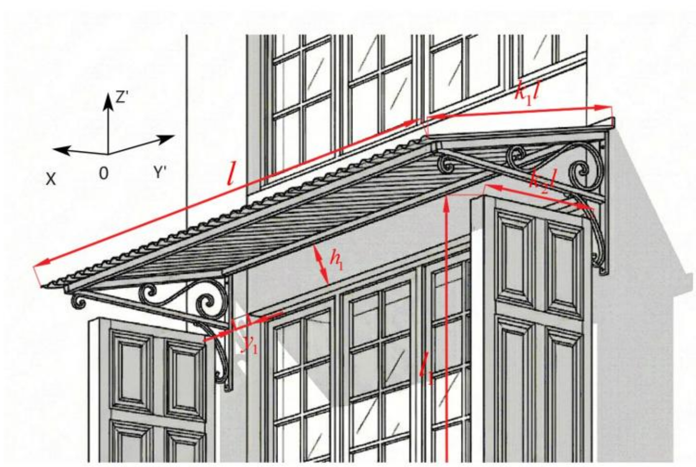

Figure 5 The schematic diagram of window physical quantity

As shown in the figure 5, we take a right-handed three-dimensional coordinate system with the geometric center of the window as the origin, x' the axis is the normal to the plane where the window is located (towards the south), z' the axis is the zenith axis, and the outer boundaries of the horizontal sunshade and the vertical sunshade can be represented as:

$$\begin{cases} x_1' = k_1 l, y_1' = y_1' \in [-Y/2, Y/2], z_1' = l/2 + h_1 \\ x_2' = k_2 l, y_2' = Y/2 + y_1, z_2' = z_2' \in [-l_1/2, l_1/2] \end{cases} \tag{7}$$

Light travels in a straight line, and the projection of sunlight on the $y'oz'$ plane of the sunshade is the projection of its outer boundary and the closed figure enclosed by the $y'oz'$ boundary of the sunshade. At this point, the incident ray vector is:

$$\vec{s}' = (\cos(\gamma_s - \gamma_1)\cos\alpha_s, \sin(\gamma_s - \gamma_1)\cos\alpha_s, \sin\alpha_s) \tag{8}$$

The expression for the incident ray passing through any point on the outer boundary of the horizontal sunshade (x_1', y_1', z_1') can be obtained:

$$\cos(\gamma_s - \gamma_1)\cos\alpha_s \cdot (x' - x_1') + \sin(\gamma_s - \gamma_1)\cos\alpha_s \cdot (y' - y_1') + \sin\alpha_s \cdot (z' - z_1') = 0 \tag{9}$$

The intersection of the incident ray and the mirror is obtained. Let $x' = 0$, and the projection point of the plane on the outer boundary of the horizontal sunshade (x'_1, y'_1, z'_1) at $y'oz'$ can be obtained $(0, y'_{o1}, z'_{o1})$.

Similarly, the projection point of the outer boundary of the vertical sunshade on the window can be obtained $(0, y'_{o2}, z'_{o2})$.

Based on the above geometric optical projection principle, the area enclosed by the orthographic projection of the sunshade onto the plane of the window is defined as the shaded region. The effective illuminated area of the window can be mathematically described as the Boolean difference between the geometric plane domain of the window and the projected shadow domain. That is, by subtracting the set formed by the projections of all sunshades from the geometric set defined by the window, the unblocked direct radiation receiving area is calculated as the effective light-receiving area A_{eff}.

Then the actual power received by the window per unit time is calculated as follows:

$$\Phi_{t1} = \eta_{In} \cdot DNI \cdot A_{eff1} \cdot (\vec{s} \cdot \vec{n}_1) \tag{10}$$

where A_{eff} is the effective light-receiving area.

For the east and west facade windows, the normal vectors of their planes are $\vec{n}_2 = (\cos\gamma_2, \sin\gamma_2, 0)$, $\vec{n}_3 = (\cos\gamma_3, \sin\gamma_3, 0)$, where γ_2 and γ_3 are the angles between the normal vectors of the planes where the two facade windows are located and the due south direction. The constraint condition is:

$$\begin{cases} \Phi_{t2} = \eta_{In} \cdot DNI \cdot (A_{eff})_2 \cdot (\vec{s} \cdot \vec{n}_2), LT \leq 12 \\ \Phi_{t2} = 0, LT > 12 \end{cases} \tag{11}$$

$$\begin{cases} \Phi_{t3} = 0, LT \leq 12 \\ \Phi_{t3} = \eta_{tn} \cdot DNI \cdot (A_{eff})_3 \cdot (\vec{s} \cdot \vec{n}_3), LT > 12 \end{cases} \tag{12}$$

that is, before 12 noon, the west-facing window cannot be directly illuminated, and after 12 noon, the east-facing window cannot be directly illuminated.

For the windows on the north facade, the normal vector of the plane they are located on is $\vec{n}_4 = (\cos\gamma_4, \sin\gamma_4, 0)$, which can only receive direct sunlight in the morning and evening near the spring equinox to autumn equinox.

The formula for calculating the radiation power received by all windows per unit time is as follows:

$$\Phi_t = \sum_i \Phi_{ti} = \eta_{In} \cdot DNI \cdot (A_{eff})_i \cdot \sum_i (\vec{s} \cdot \vec{n}_i) \tag{13}$$

The constraint condition for each facade window to receive direct sunlight without sunshades is:

$$\gamma_s \in (\gamma_i - \pi/2, \gamma_i + \pi/2) \tag{14}$$

Based on (14), the critical time for receiving light can be determined by reversing the solar azimuth angle γ_s, obtaining the range of local time LT.

In summary, the total solar radiation energy received by a building during a day can be calculated using the following formula:

$$Q = \sum_{i} \int_{t_i}^{t_{i+1}} \Phi_t dt \tag{15}$$

Finally, the effective light receiving area is solved by discretization and polygon Boolean operation algorithm. In the previous theory, we obtained the area enclosed by the projected boundary of the outer boundary of the sunshade onto the window plane, which is the shaded region. The effective light-receiving area A_{eff} can be calculated by performing Boolean subtraction between the window's geometric plane domain and all projected shadow domains using MATLAB's polyshape library.

2.2 Model solution and result analysis

University 1 as an example, at a latitude of approximately 28 °N, the academic building is 8m high, the window transmittance is constant at 0.75, the size is set as a rectangle 2m long and 1.5m high, and it is uniformly distributed on the wall.

2.2.1 Sensitivity analysis of geometric parameters of sun visors

To determine the key decision variables for sunshade design, according to viewpoint iii, we first conducted a sensitivity analysis on the geometric parameters of the south facade sunshade based on data from the Autumn Equinox, including gap (distance from the window edge), depth (length extending beyond the building), and extension (length extending beyond the window edge). The results are shown in the figure 6:

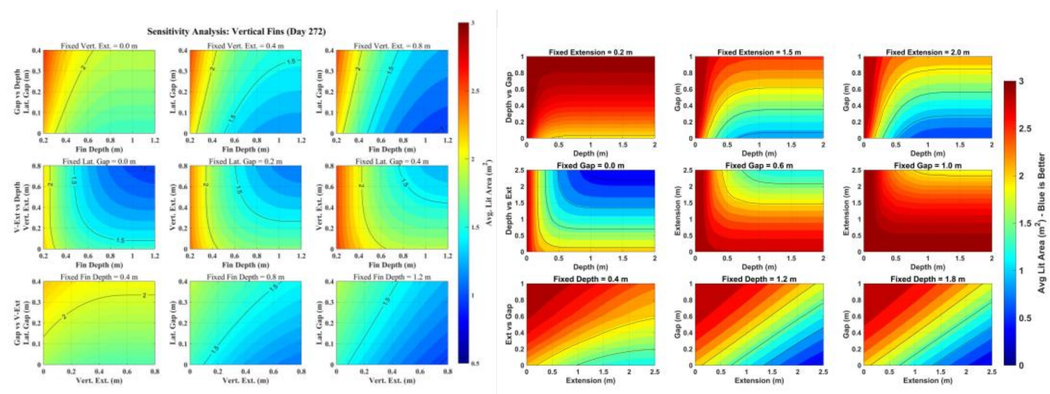

Figure 6 Sensitivity analysis of horizontal and vertical sunshade parameters

Depth exhibits the highest sensitivity and is the dominant factor determining shading effectiveness. Once a critical threshold is reached, the marginal contribution of changing extension and gap to the average effective light-receiving area decreases significantly.

2.2.2 Decoupling Analysis of Shading Effectiveness at Different Times

To investigate the time adaptability of different types of sunshades, we fixed the gap to 0 and simulated the independent shading effectiveness of horizontal and vertical sunshades at four time steps from sunrise to noon. Early morning (near sunrise): Solar azimuth angle's absolute value is large (eastward), altitude angle is small. Vertical sunshade can block side-incident light effectively, while horizontal sunshade needs large extension for shading.

Noon: Solar azimuth angle approaches 0 (due south), altitude angle peaks. Horizontal sunshade only needs small depth to cover window's upper area, vertical sunshade is almost ineffective.

Conclusion: A single sunshade can't meet all-day shading needs. Combined shading, installing horizontal and vertical sunshades near the window edge with $d_{gap} = 0$ and length matching window size, is the optimal choice under cost constraints.

2.2.3 Optimization of Total Solar Radiation

We established a multivariate optimization model to optimize the orientation of windows on each facade γ_i, the depth of each sunshade. The optimization targets include the total sunshade area S and the average total solar radiation energy in summer $\bar{Q}$.

Decision variables:

Orientation angle of windows on each facade γ_i, depth of each shading panel.

Objective function:

Minimize the total shading panel surface area S;

Minimize the average total solar radiation energy in summer $\bar{Q}$.

Constraints:

Actual incident power of the main light-receiving surface (e.g., east-facing in summer) $\Phi_t < 0.01 * \Phi_0$ (Incident power without sunshade);

For non-primary light-receiving surfaces, the sunshade area should be reduced first, provided that basic shading is met.

According to viewpoint i, the main radiation in summer comes from the east facade in the morning and the north facade in the morning and evening.

For the east facade, the normal incident power is extremely high due to the small solar altitude and azimuth angles in the early morning during summer. Simulations show that the optimal depth for the horizontal sunshade is 1.5m, and for the vertical sunshade it is 0.7m.

When the window is rotated from due east to south 15 °, with a slightly extended horizontal sunshade, the minimum radiant power can be reduced to 0.53 times that of the unrotated state. This demonstrates the synergistic effect of geometric orientation optimization and sunshade component design.

For the south facade, the solar altitude angle received by the south facade is large in summer, resulting in low normal incident power. Simulations show that a horizontal sunshade depth of 0.22m and a vertical sunshade depth of 0.22m achieves good shading. Meanwhile, south-facing windows are not sensitive to rotation in summer.

For the north-facing facade, the optimal horizontal sunshade depth is 0.4m and the vertical is 0.95m. However, in the early morning, as there is a larger angle between the sunshade and the azimuth angle and the azimuth angle is smaller, it's highly sensitive to rotation. When the window rotates from due north to west 15°, the minimum radiant power can be reduced to 0.01 times that of the unrotated state, significantly cutting the solar radiation power received on the north side in the early morning. Meanwhile, the depth requirement for horizontal sunshades also decreases.

2.2.4 Performance Verification

The figure below shows the time distribution curve of the incident solar power during the critical period around the summer solstice based on the optimal parameters. Dashed lines represent the no-shade reference group and solid lines represent the optimized shade group. The design successfully intercepted 86% of the radiant energy.

At the same time, the remaining part of the radiation is mainly received by the east and west facades in the morning and evening. The direction of the cantilevered sunshade or windows has obvious benefits for the boundary of sunshade. Therefore, it is recommended to introduce high-reflectivity glass, movable blinds, etc. as dynamic adjustment means, or configure tall trees for ecological sunshade in the surrounding area of the building, so as to block low-angle incident light in the morning and evening.

2.2.5 Comparison with traditional models

As shown in the figure below, traditional models often ignore radiation changes during non-noon periods, resulting in severe shading failure in the morning and evening periods (when the solar altitude angle is low but the azimuth angle is large), especially for east-west facades. Our model is based on projection geometry for dynamic analysis of the entire day, and introduces vertical sunshades to prevent sunshade failure and reduce the solar radiation power throughout the day. Geometric parameters of each facade window and sun visor is shown in table 1.

Table 1 Geometric parameters of each facade window and sun visor

Orientation	Horizontal sunshade			Vertical sunshade			Deflection angle (°)
	Length(m)	Depth(m)	Distance from the edge of the window(m)	Length(m)	Depth(m)	Distance from the edge of the window(m)	

North facade	2	0.4	0	1.5	0.95	0	15
East facade	2	1.5	0	1.5	0.7	0	105
South facade	2	0.22	0	1.5	0.22	0	180
West facade	2	1.5	0	1.5	0.7	0	255

3 Conclusion

This section systematically elucidates the complex coupling between solar trajectory, atmospheric attenuation effects, and building shading components by constructing a solar radiation geometric projection model. The polygonal Boolean operation algorithm precisely calculated the effective sun-exposed areas of each facade, validating the superiority of composite designs combining horizontal and vertical louvers in addressing dynamic solar radiation impacts throughout the day. However, the current model primarily focuses on geometric shading analysis of direct radiation, simplifying the contributions of atmospheric scattering and ground-reflected radiation in complex environments. Furthermore, the model employs linear assumptions for material optical properties, failing to fully account for the nonlinear Fresnel effect where glass transmittance varies with incident angle. Future research should focus on incorporating full-spectrum radiation coupling mechanisms and integrating multi-objective genetic algorithms with real-time dynamically adjustable shading systems to enhance environmental control resilience in buildings under variable climatic conditions.

References

[1] Niu Z, Ji R, Wang G, et al. PolygonTailor: A Parallel Algorithm for Polygon Boolean Operations in IC Layout Processing[J]. Algorithms, 2026, 19(2):145-145.

[2] Zhang Y, Lu Y, Wang Y, et al. How does sun shading affect street commercial vitality? Evidence from street view images[J]. Sustainable Cities and Society, 2026, 136107082-107082.

[3] Yi HD, Choi S, Kim WD, et al. Quantifying urban building shading effect for data-driven building energy modeling[J]. Building and Environment, 2026, 289114011-114011.

[4] Zhou Z, Dong L, Jiao R, et al. Effects of building shading on outdoor adaptive thermal comfort and the development of predictive models[J]. Building and Environment, 2026, 288113983-113983.

[5] Wang H, Li W, Fazilati A M, et al. Review of simulation modeling and artificial intelligence, such as artificial recurrent neural network, deep learning, regression, and classification for shading devices in buildings[J]. International Communications in Heat and Mass Transfer, 2025, 169(PE): 109873-109873.

[6] Khan F, Sen S. Thermal performance of jointed plain concrete pavements in urban areas considering shade from buildings[J]. Discover Civil Engineering, 2025, 2(1): 179.

[7] Yi Yang, Xiao Yingxiong, Yu Ke. Establishment and Numerical Simulation of a Microscopic Model for Arbitrary Polygonal Aggregate Concrete[J]. Journal of Shandong University (Engineering Edition), 2025, 55(01): 97-107.
[8] Feng Xiaolong, Su Maojang, Tong Weihua, et al. Generalized Polygonal Boolean Operations with Curved Edges [J/OL]. Journal of Computer-Aided Design and Graphics, 1-12 [2026-03-06].
[9] Zhang, Y. L., Wang, J. R., Wu, Q. Q. Research and implementation of efficient Boolean operation technology for complex 3D solids [J]. Computer Applications and Software, 2025, 42(01): 249-257+327.
[10] Zheng W, Wu H, Xu G, et al. Feature-preserving quadrilateral mesh Boolean operation with cross-field guided layout blending. Computer Aided Geometric Design, 2024, 111102324.